Comparison of Surface Radio Refractivity Variability in the Northern and Southern of Quebec, Canada

Yamina Bettouche[1], Huthaifa obeidat[2], Mahmood Mosleh[3], Alli Alabdullah[4], Basile L. Agba[1], ammar kouki[5], and Raed A Abd-Alhameed[4]

[1]École de Technologie Supérieure
[2]Jerash University
[3]Middle Technical University
[4]University of Bradford
[5]Ecole de technologie supérieure

November 22, 2022

Abstract

A 39 years of archived meteorological data measured at two stations located in the northern and southern parts of the Quebec, Canada is used to estimating the surface refractivity and its dry and wet components. The results of the comparison of the obtained estimates showed that for all months the values of the dry component are higher in the northern part, whereas that the values of the wet component are higher in the southern part. Due to this, for several months of the year, the values of the surface refractivity are higher in the northern part and for the remaining months in the southern part. Moreover, in both parts, August is the month where the highest values of the surface refractivity were recorded. For this month, the slope of the surface refractivity trend in the northern is several times higher than that in the southern part.

Comparison of Surface Radio Refractivity Variability in the Northern and Southern of Quebec, Canada

Y. Bettouche[1], H. A. Obeidat[2], Mahmood F. Mosleh[3], Ali AlAbdullah[4], B.L. Agba[1], A. B. Kouki[1], and R.A. Abd-Alhameed[4]

[1]École de Technologie Supérieure, Lacime, Montréal, Canada
[2]Faculty of Engineering, Jerash University, Jordan
[3]College of Electrical Engineering Techniques, Middle Technical University, Baghdad, Iraq
[4]Faculty of Engineering and Informatics, University of Bradford, Bradford, Richmond Street, UK

Corresponding author: Huthaifa Obeidat (h.obeidat@jpu.edu.jo)

Key Points:

- The study shows that the dry (N_d) and wet (N_w) components of the surface refractivity have different mean monthly variability in North and South of Quebec. For all months, the values of N_d are higher in the northern part, whereas the values of N_w are higher in the southern part.

- Since the water vapour pressure in Montreal undergoes more significant variation than in Kuujjuaq, for the wet component, there is a significant difference between the variations observed in Montreal than in Kuujjuaq.

- The slope of the estimated mean yearly trends of the surface refractivity in both parts is positive. However, the slope of the trend in the northern is several times higher than that in the southern part.
- The direct smoothing, a forecasting technique which is efficient computationally has been used to estimate the future values of N in Kuujjuaq.

Abstract

A 39 years of archived meteorological data measured at two stations located in the northern and southern parts of the Quebec, Canada is used to estimating the surface refractivity and its dry and wet components. The results of the comparison of the obtained estimates showed that for all months the values of the dry component are higher in the northern part, whereas that the values of the wet component are higher in the southern part. Due to this, for several months of the year, the values of the surface refractivity are higher in the northern part and for the remaining months in the southern part. Moreover, in both parts, August is the month where the highest values of the surface refractivity were recorded. For this month, the slope of the surface refractivity trend in the northern is several times higher than that in the southern part. The obtained results show that the performance of the used direct smoothing forecasting technique depends on the deviation between the values of *N* of the current year and the previous year.

1. Introduction

For transmitting audio or/and video data from the transmitter to receiver the terrestrial fixed radio links operating at microwave frequencies on line-of-sight (LOS) are frequently used (B. R. Bean, 1962; Bogucki & Wielowieyska, 2009; Grabner, Kvicera, Pechac, & Mudroch, 2010). However, the performance of the transmission depends on the used equipment, as well as the values of the meteorological parameters present in the transmission medium (troposphere in this case). The troposphere is the region of the atmosphere extending from the surface of the Earth up to a height of 8-10 km at polar altitudes, 10-12 km at moderate latitudes and up to 18-19 km at the equator (Adediji, Ajewole, Falodun, & Oladosu, 2007; Grabner, Kvicera, Pechac, & Jicha, 2012). The temperature, pressure and relative humidity are the main parameters whose variability has an important impact on the quality of the propagation of radio waves (Ali, Malik, Alimgeer, Khan, & Ali, 2012; Grabner & Kvicera, 2003; ITU, 2015; Kablak, 2007; Priestley & Hill, 1985). Therefore, in the design of communication systems, it is necessary to take into account this variation. The atmospheric refractivity *N* is generally used as a metric for this purpose. ITU provides a procedure to find the value of *N* (ITU, 2015) when the correspondent meteorological parameters are known.

Authors in (B. Bean & Cahoon, 1961) showed that there is a high correlation between the surface refractivity and the field strength; through the magnitude of the electromagnetic field which will induce a voltage that will be the input signal for the receiver (Adekunle Titus Adediji, 2017). In (AbouAlmal et al., 2015) authors used local surface meteorological data measured over seventeen years from six stations and one radiosonde to present and compare the surface refractivity profiles in the United Arab Emirates (UAE). The obtained results were different from the values provided by the ITU. Hence, there is a need to explore always locally measured data. However, this study did not analyse the trend of the surface refractivity over the considered period. In (Adediji, 2017) author presented the obtained results of the variability of surface refractivity estimated based on two years on meteorological data measured at three stations located South-Western, North-Central and South-Eastern of Nigeria. The analyzed period was limited only to two years, which is not enough to draw general conclusions. In (Ayantunji, Okeke, & Urama, 2011) authors presented an analysis of seasonal variation of surface refractivity over Nigeria; however, data of only two years had been used.

Other metrics are used to evaluate the quality of the propagation, including refractivity gradient (dN) in the first 1 km above the surface (Valma, Tamosiunaite, Tamosiunas, Tamosiuniene, & Zilinskas, 2011) (B. Bean, Frank, & Lane, 1963; Lane & Bean, 1963) and the equivalent gradient (G_e) (Misme, 1960).

Authors in (Valma et al., 2011) studied the variations of radio refractivity and its vertical gradient in Lithuania, they found that the radio refractivity and its vertical gradient could change as the weather suddenly becomes significantly colder. In (Lane & Bean, 1963) a correlation coefficient of 0.7 between the field strength for the propagation of VHF (very high frequency) and dN was obtained, however, the surface refractivity N finds a wide usage since it can be easily evaluated from the measurements of temperature, pressure, and relative humidity.

In this study, the meteorological data collected over the last 39 years from one station located in the Northern part and another to the Southern part of Quebec are used in the formulae provided by ITU recommendations to estimate the surface refractivity. The main contributions of this paper are:

1) To give a detailed comparison of the variability of surface refractivity in the Northern and Southern parts of Quebec. This is motivated by the fact that the two parts are located in different climatic zones.
2) To propose a forecasting technique which has not only a good performance but also requires is not little calculations.

The organisation of the paper is as follows: Section II describes the used approach to estimate surface refractivity. While Section III presents an analysis of the obtained results. Finally, the conclusion is drawn in Section IV.

2. Used Approach

2.1 Data

The used meteorological data are measured from the Kuujjuaq and Montreal stations. The Kuujjuaq station is located in the Northeast of Quebec at 58.1º latitude and -68.42 º longitude, with an altitude of 39.9 m above sea level. The Montreal station is located in the Southeast of Quebec at 45.7º latitude and -73.74 º longitude, with an altitude of 32.1 m above sea level. The government of Canada provides local climatic parameters (temperature, dew temperature, humidity, pressure, etc.) stored in raw CSV format (Canada, 2019). These files are converted into Excel files for further processing. An example of this file is shown in Table 1.

Table 1: *A sample of the collected data for 2013.*

Date	Time	Temperature, t (°C)	Dew Temperature, tr (°C)	Relative Humidity, H (%)	Pressure, P (kPa)
01-08-2013	00:00	11.5	9.1	85	100.74
	01:00	11.2	9.2	87	100.72
	…	…	…	…	…
	23:00	8.5	6.9	90	100.66
…	…	…	…	…	…
31-08-2013	00:00	3.2	0.3	81	100.12
	01:00	2.9	-0.6	78	100.11
	02:00	1.8	0	88	100.12
	…	…	…	…	…
	23:00	4.3	0.2	75	100.89

2.2 Methodology

It is well known that the surface refractivity has dry and wet components. These components are determined by (ITU, 2015):

$$N_d = 77.6\frac{P_d}{T} \qquad (1)$$

where *T* is the absolute temperature (*K*), P_d is the dry atmospheric pressure (hPa) which is given by:

$$P_d = P - e \qquad (2)$$

where *P* is the total atmospheric pressure (hPa) and *e* is the water vapour pressure (hPa).

$$N_w = 72\frac{e}{T} + 3.75\frac{e}{T^2} \qquad (3)$$

As seen from Equation 3, the dry component varies with both pressure and temperature. The wet component as seen from Equation 5 depends on the values of humidity and temperature. The water vapour pressure in *hPa* is determined by (ITU, 2015):

$$e = \frac{He_s}{100} \qquad (4)$$

where *H* is the relative humidity (%), and e_s is the saturation vapour pressure (hPa) determined by:

$$e_s = EF_{water} \cdot a \cdot \exp\left[\frac{bt - \frac{t^2}{d}}{t + c}\right] \qquad (5)$$

where *t* is the temperature (^{o}C), $a = 6.1121$; $b = 18.678$; $c = 257.14$; $d = 234.5$, and:

$$EF_{water} = 1 + 10^{-4}[7.2 + P(0.032 + 5.9 \times 10^{-6}t^2)] \quad (6)$$

3. Results And Analysis

The available measured data at Kuujjuaq and Montreal stations are used to estimate the surface refractivity and its dry and wet components. Note that in reference (Bettouche et al., 2019) the authors have used only data collected at the Kuujjuaq. This manuscript completes the previous work by comparing the variations of *N* in northern (Kuujjuaq) and southern (Montreal) parts of Quebec. We also use a forecasting technique to estimate future values of *N* in Kuujjuaq. This has not been done in the previous paper.

3.1 Analysis of the surface refractivity (N)

The refractivity at some altitude h above the sea level, N and the sea level refractivity, N_0 are related by (Adediji, 2017):

$$N = N_0 e^{\left(\frac{-h}{h_0}\right)} \qquad (7)$$

where h is the height of the earth's surface above sea level and h_0= 9.5 km. Considering the altitudes of Kuujjuaq at Montreal stations and Equation 9 there will not be a noticeable difference between the values of N and N_0. For this reason, our analysis will be based on the values of N.

Figure 1 shows the mean monthly variations of N_d for the considered stations. From this figure, it is clear that the values of N_d in Kuujjuaq for all months are higher than the correspondent values in Montreal; this is because the dry atmospheric pressure, which determines the value of the dry component, is always higher in Kuujjuaq than in Montreal, in the figure, it can be seen that the values are higher in winter season compared to other seasons, because in winter the dry atmospheric pressure which determines the value of the dry component is always higher than in other seasons. The maximum and minimum values of N_d are shown in the figure. As seen, in Kuujjuaq the maximum and minimum values are 312.7 N-units (in February) and 270.5 N-units (in July). It worth mentioning that the maximum values in Kuujjuaq and Montreal occurred in February and January respectively, since the maximum value of the dry atmospheric pressure occurs in these months.

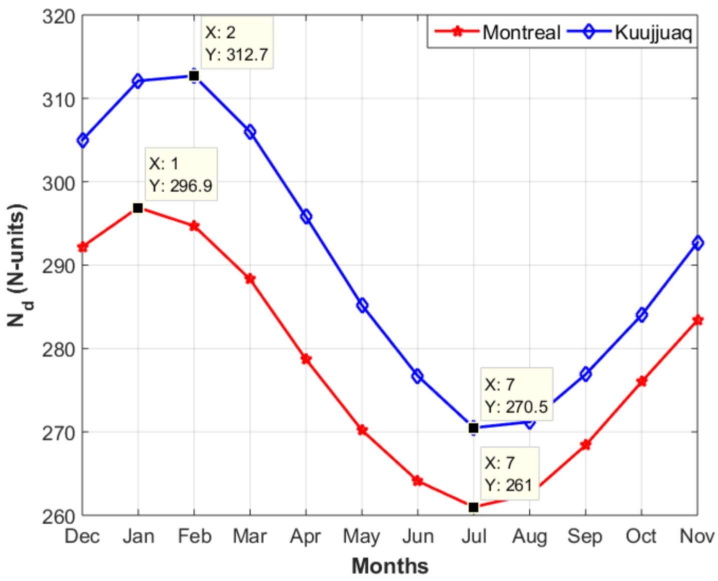

Figure 1: Mean monthly variations of dry components

Figure 2 shows the mean monthly variations of N_w for the two stations. From Figure 2, we see that for N_w the values in Montreal for all months are higher than the correspondent values in Kuujjuaq, the value of the wet component is mainly determined by the water vapour pressure, in Kuujjuaq the value of the water vapour pressure is always lower than in Montreal. The maximum and minimum values of N_w are shown in the figure. In the figure, values are always higher in summer compared to other seasons because in summer the water vapour pressure, which determines the value of the wet component, is always higher than other seasons. It worth mentioning that the minimum values in Kuujjuaq and Montreal occurred in February and January respectively, since the minimum value of the dry atmospheric pressure occurs in these months.

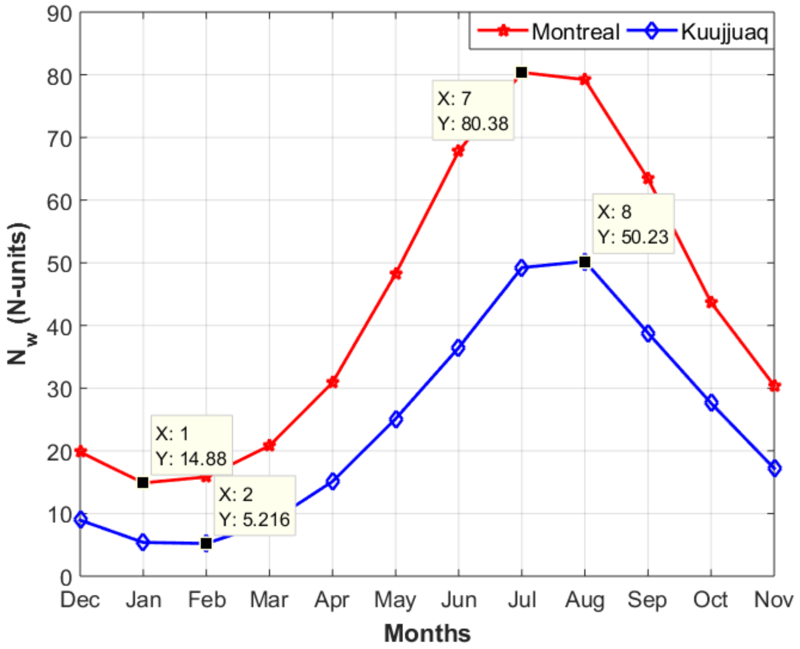

Figure 2: Mean monthly variations of wet components

Table 2 shows the values of the difference between the maximum and minimum values of N_d and N_w in Montreal and Kuujjuaq.

Table 2: *Difference between the maximum and minimum values of N_d and N_w in Montreal and Kuujjuaq*

Station	ΔN_d	ΔN_w
Montreal	35.9	65.5
Kuujjuaq	42.2	45.014

From Table 2 it can be concluded that in Montreal there is a relatively significant difference between the variations of N_d and N_w in comparison to the same difference observed in Kuujjuaq. For the wet component, there is a significant difference between the variations observed in Montreal than in Kuujjuaq. This is because the water vapour pressure in Montreal undergoes more significant variation in Montreal than in Kuujjuaq. Table 3 shows the correlation between mean monthly values of *N* and temperature as well as and water vapour.

Table 3: *the correlation between mean monthly values of N and temperature as well as and water vapour*

Month	Montreal			Kuujjuaq		
	T (K)	*e* (hPa)	*P* (hPa)	*T* (K)	*e* (hPa)	*P* (hPa)
Dec	0.13	0.32	0.58	-0.81	-0.65	0.56
Jan	-0.46	-0.28	0.74	-0.92	-0.81	0.71
Feb	-0.07	0.17	0.72	-0.85	-0.70	0.44
Mar	0.06	0.53	0.50	-0.74	-0.65	0.26
Apr	0.14	0.84	0.01	-0.50	-0.27	0.62

May	0.45	0.93	0.14	0.17	0.53	0.22
Jun	0.44	0.97	-0.07	0.44	0.79	0.34
Jul	0.37	0.96	-0.05	0.71	0.96	-0.18
Aug	0.51	0.95	-0.04	0.61	0.95	0.08
Sep	0.84	0.97	0.13	0.59	0.91	0.11
Oct	0.89	0.97	0.22	0.59	0.79	0.39
Nov	0.66	0.85	0.12	-0.23	-0.02	0.70

Analysis of the data shown in Table 3 and the variations of wet components shown in Figure 2 show that the difference between the values of N_w for months with a high correlation coefficient between N and e is higher than the months with less value of the same correlation coefficient. Therefore, the humidity has a more impact on the value of refractivity in the South than in the North. Figure 3 shows the mean monthly variations of N for the two stations.

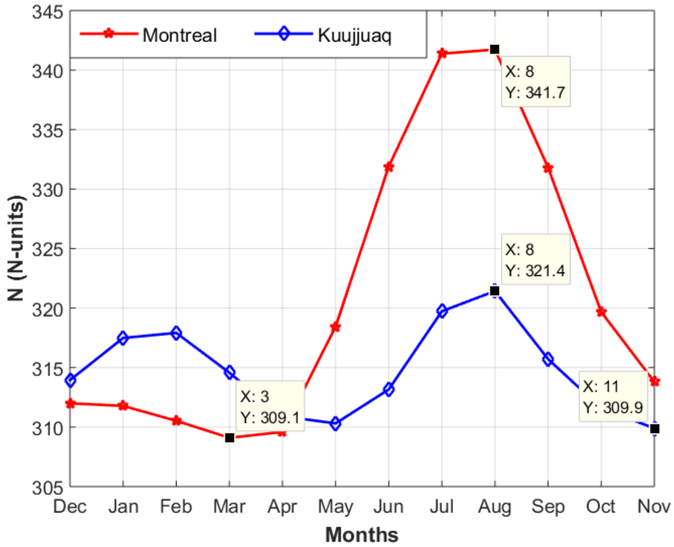

Figure 3: Mean monthly variation of refractivity.

As seen in Figure 3, the values of N in Kuujjuaq are higher than the values in Montreal for the months: December, January, February, March, and April (the majority of winter and spring seasons). While for the majority of summer and autumn months, the values of N tend to be higher in Montreal. These variations are due to the variations of N_w. As it is seen from Fig.2 for the months from May to November the values of N_w in Montreal are much higher than the values for the months from December to April. Also from Figure 4, it is clear that the relative contribution of N_w to N is higher for the months from May to November in both locations. In Montreal, the highest relative contribution of N_w to N lies in July (23.55%) while the lowest contribution (4.773%) is found to be in January. In Kuujjuaq the maximum and minimum relative contributions lie in August (15.63%) and February (1.641%) respectively. However, for each station the relative contribution of N_w to N for the months of July and August are similar.

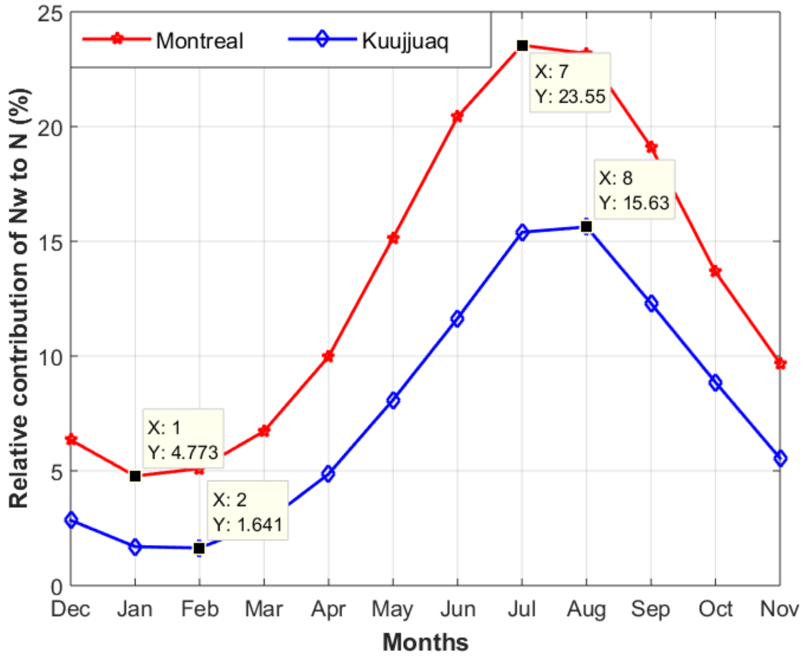

Figure 4: Mean monthly relative contribution of N_w to N

Figure 5 shows the mean yearly variation of refractivity and its linear trend from 1981 to 2019 in Montreal and Kuujjuaq. Here and in the rest of this document, it will be assumed that the variable x represents a specific year in the analyzed period. The linear trend for Montreal follows a $0.015x + 320$ while for Kuujjuaq it follows $0.0048x + 310$ as shown in Figure 5. Therefore, starting from 1981, each year, N increases by 0.015 and 0.0048 N-unit in Montreal and Kuujjuaq respectively. Thus, the increase of N trend in Montreal is significantly greater than in Kuujjuaq.

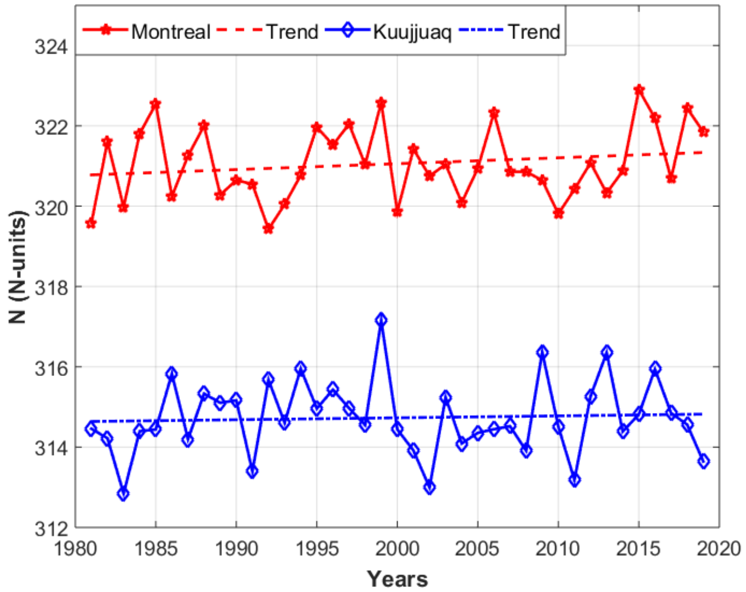

Figure 5: Mean yearly variation of refractivity.

Figure 6 shows the mean yearly cumulative distribution over the analyzed period for the two stations. Analysis of distributions shown in Figure 6 shows that for a percentage of time less than 10%, the worst location (location with highest values of N) is Kuujjuaq. For all remaining time percentages, the worst location is Montreal.

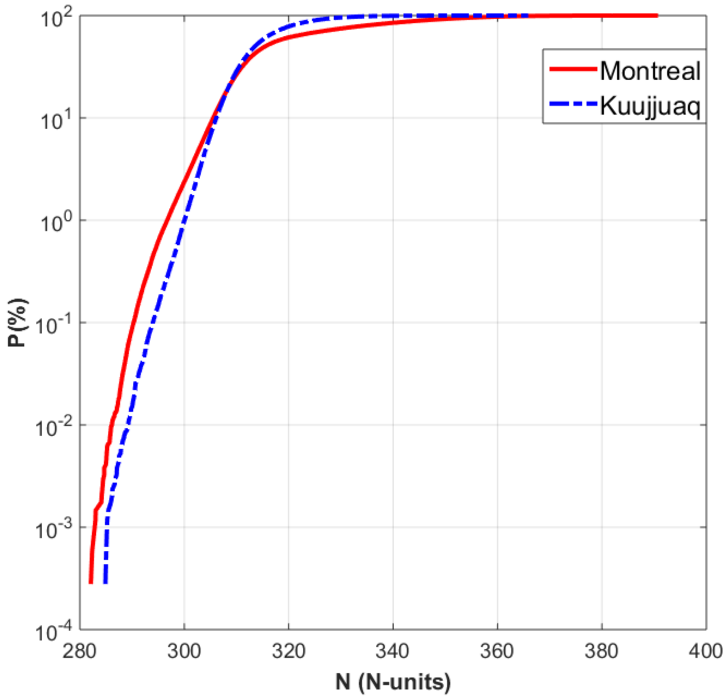

Figure 6: Mean yearly PDF of N.

3.2 Analysis of refractivity for the worst month

For each station, we have selected the month with the maximum value of N (worst month). This month for both stations is August. Figure 7 shows the corresponding variations of N and their trends over the analyzed period.

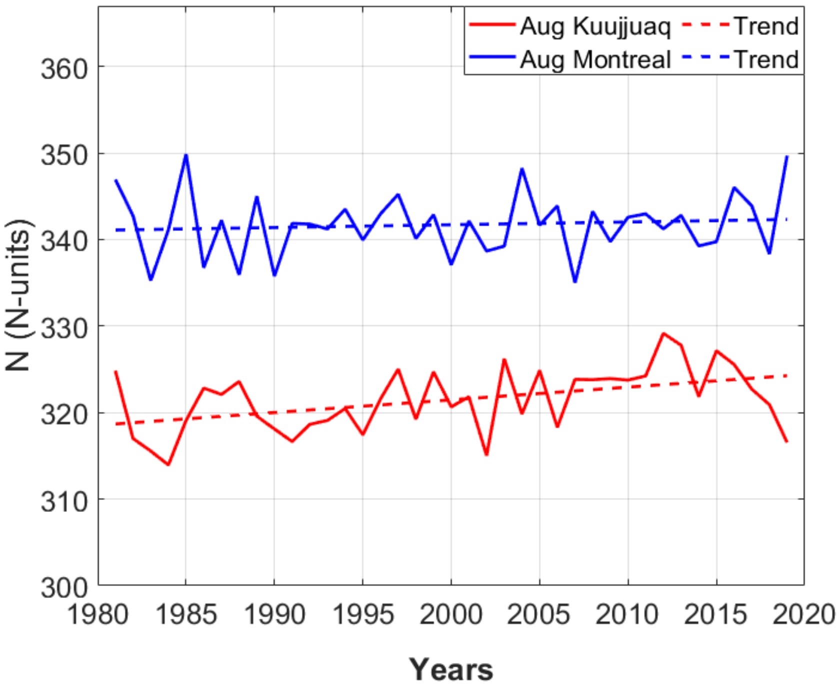

Figure 7: Average yearly variations of N for the worst month.

The values of *N* in Montreal are significantly higher than in Kuujjuaq. Our analysis shows that for both stations the variance has a minimum value when the variation of *N* is modelled as a linear trend process rather than a constant process. The equations for linear trends shown in Fig.7 are 0.1414x+318.8 and 0.0348x+341 for Kuujjuaq and Montreal respectively. These equations show that in the northern part of Quebec there is a relatively high increase (0.1414 N-unit each year) in comparison to the southern part where the increase is only 0.0348 N-unit each year.

Since the station Kuujjuaq has the highest slope for the variation of *N* in the rest of this section, we propose a procedure to estimate future values of *N*. The procedure is based on the use of the so-called direct smoothing (Douglas, Lynwood, & John, 1990). The main advantage of direct smoothing is computationally efficient. According to this forecasting technique, the new model parameters are obtained from the previous parameters by adding the current period's forecast error weighed with some coefficient. The forecast value of *N* at some period T is (Douglas et al., 1990):

$$N_f(T) = a_1(T) + a_2(T) \tag{8}$$

where $a_1(T)$ and $a_2(T)$ are the model parameters determined for the period T:

$$\begin{cases} a_1(T) = a_1(T-1) + a_2(T-1) + \left(1-\beta^2\right)e(T) \\ a_2(T) = a_2(T-1) + \left(1-\beta\right)^2 e(T) \end{cases} \tag{9}$$

and e(T) is the forecast error (The difference between the observed value N(T) and the forecast for that value $N_f(T)$

$$e(T) = N(T) - N_f(T) \tag{10}$$

Note that in order to estimate $N_f(T)$, the initial values of $a_1(0)$ and $a_2(0)$ are required. In our case, we consider $a_1(0)$ and $a_2(0)$ as intercept and slope of the obtained linear trend based on the first 25 years historical data of N. We get: $a_1(0) = 318.828$ and $a_2(0) = 0.1263$.

The variable β in equation (9) is the discount factor, whose value lies in the interval $0< \beta < 1$. In this case to select the optimal value of β we use the value which yields the minimum value of sum of the squares of the deviations between the observed values of *N* and the correspondent forecasts for the remaining 14 years historical data when β is set in the interval 0.1 to 0.9 with a step 0.1. Remember that the in analysis data collected over a period of 39 years are used. Since data for the first 25 years have been used for estimating the initial values of the model parameters it will remain only data for 14 years. The data for these remaining years are used for estimating the forecast. We found that the optimal value of β is 0.6. For this value of β figure 8 shows the observed values and forecasts obtained using the described procedure above for the remaining last 14 years of the analysed period.

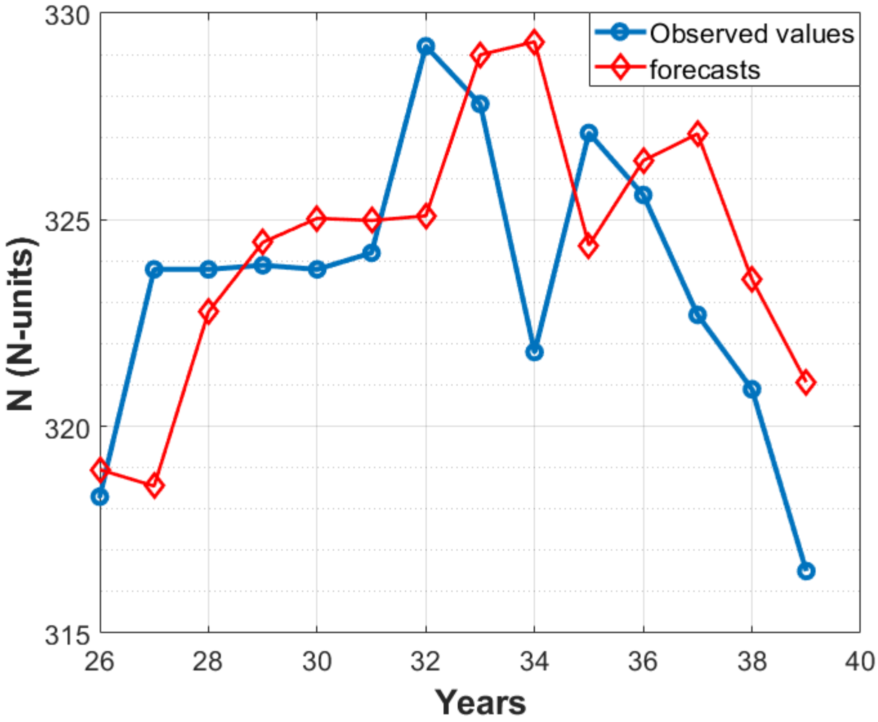

Figure 8: Observed of N and forecasts for the last 14 years of the analysed period.

From Figure 8 we can conclude the forecasts are relatively far from the observed values for years where the observed value is far away from the previous year. Thus the performance of the used forecasting technique depends on the deviation between the values of N of the current year and the previous year.

4. Conclusion

The main findings in the performed study are: The dry component is the main component of *N* in North and South of the Quebec and that for all months; values of *N* are higher in the northern part. For the wet component, it was found that the values of *N* are higher in the southern part for all months. The highest values of *N* lie in summer, particularly in August month in the North, as well as in the South. However, for this month, the slope of the surface refractivity trend in the northern is several times higher than that in the southern part, whereas the intercept in the south is higher than in the north. Also, a direct smoothing as a forecasting technique has a relatively good performance.

Acknowledgements

All measured data are available in the following link:

https://zenodo.org/record/3607942#.Xh3VScgzbIU

References

AbouAlmal, A., Alhassan, H., Obeidat, H., Abusitta, M., Abd-Alhameed, R., Jones, S., & Al-Ahmad, H. (2015). *Surface refractivity profile and validation of measurements in Arabian Gulf region.* Paper presented at the 2015 Loughborough Antennas & Propagation Conference (LAPC).

Adediji, A. (2017). Reduced-to-sea-level value of microwave radio refractivity over three stations in Nigeria. *Nigeria Journal of Pure and Applied Physics, 7*(1), 19-25.

Adediji, A., Ajewole, M., Falodun, S., & Oladosu, O. (2007). Radio refractivity measurement at 150 m altitude on TV tower in Akure, South West Nigeria. *Journal of Engineering and Applied Sciences, 2*(8), 1308-1313.

Adekunle Titus Adediji, S. O. A. a. J. S. O. (2017). Variability of Microwave Radio Refractivity and Field Strength over Some Selected Locations in Nigeria. *Physical Science International Journal, 14*(3).

Ali, S., Malik, S. A., Alimgeer, K. S., Khan, S. A., & Ali, R. L. (2012). Statistical estimation of tropospheric radio refractivity derived from 10 years meteorological data. *Journal of atmospheric and solar-Terrestrial physics, 77*, 96-103.

Ayantunji, B., Okeke, P., & Urama, J. (2011). Seasonal variation of surface refractivity over Nigeria. *Advances in space Research, 48*(12), 2023-2027.

Bean, B., & Cahoon, B. (1961). Correlation of monthly median transmission loss and refractive index profile characteristics. *J. Res. NBS, 65*(1), 67-74.

Bean, B., Frank, V., & Lane, J. (1963). A radio meteorological study, part II. An analysis of VHF field strength variations and refractive index profiles. *J. Res. NBS D, 67*, 597-604.

Bean, B. R. (1962). The radio refractive index of air. *Proceedings of the IRE, 50*(3), 260-273.

Bettouche, Y., Obeidat, H., Agba, B., Kouki, A., Alhassan, H., Rodriguez, J., . . . Jones, S. (2019). Long-Term Evolution of The Surface Refractivity for Arctic Regions. *Radio Science, 54*(7), 602-611.

Bogucki, J., & Wielowieyska, E. (2009). Empirical season's fadings in radio communication at 6 GHz band. *Journal of telecommunications and information technology*, 48-52.

Canada, G. o. (2019). Données climatiques historiques. Retrieved from http://climat.meteo.gc.ca/

Douglas, C. M., Lynwood, A. J., & John, S. (1990). Forecasting and time series analysis. *McGraw-Hill, Inc, 2nd Edition. Columbus, OH, USA. Estévez PA, Tesmer M., Perez CA, and Zurada JM (2009). Normalized mutual information feature selection. IEEE Transactions on Neural Networks, 20*(2), 189-201.

Grabner, M., & Kvicera, V. (2003). Clear-air propagation modeling using parabolic equation method. *RADIOENGINEERING-PRAGUE-, 12*(4), 50-54.

Grabner, M., Kvicera, V., Pechac, P., & Jicha, O. (2012). *Parameters of vertical profiles of temperature humidity and refractive index of air in the lowest troposphere.* Paper presented at the Proc. of 9th International Symposium on Tropospheric Profiling (ISTP).

Grabner, M., Kvicera, V., Pechac, P., & Mudroch, M. (2010). *Multipath fading measurement and prediction on 10 GHz fixed terrestrial link.* Paper presented at the 15th Conference on Microwave Techniques COMITE 2010.

ITU. (2015). *ITU-R P.453-11: The radio refractive index: its formula and refractivity data*. Retrieved from Geneva:

Kablak, N. (2007). Refractive index and atmospheric correction to the distance to the Earth’s artificial satellites. *Kinematics and Physics of Celestial Bodies, 23*(2), 84-88.

Lane, J., & Bean, B. (1963). A radio Meteorological Study, Part 1. *Existing Radio Meteorological Parameters*, 589-604.

Misme, P. (1960). Models of the atmospheric radio refractive index. *PROCEEDINGS OF THE INSTITUTE OF RADIO ENGINEERS, 48*(8), 1498-1499.

Priestley, J., & Hill, R. (1985). Measuring high-frequency humidity, temperature and radio refractive index in the surface layer. *Journal of atmospheric and oceanic technology, 2*(2), 233-251.

Valma, E., Tamosiunaite, M., Tamosiunas, S., Tamosiuniene, M., & Zilinskas, M. (2011). Variation of radio refractivity with height above ground. *Elektronika ir Elektrotechnika, 111*(5), 23-26.

Figure 1.

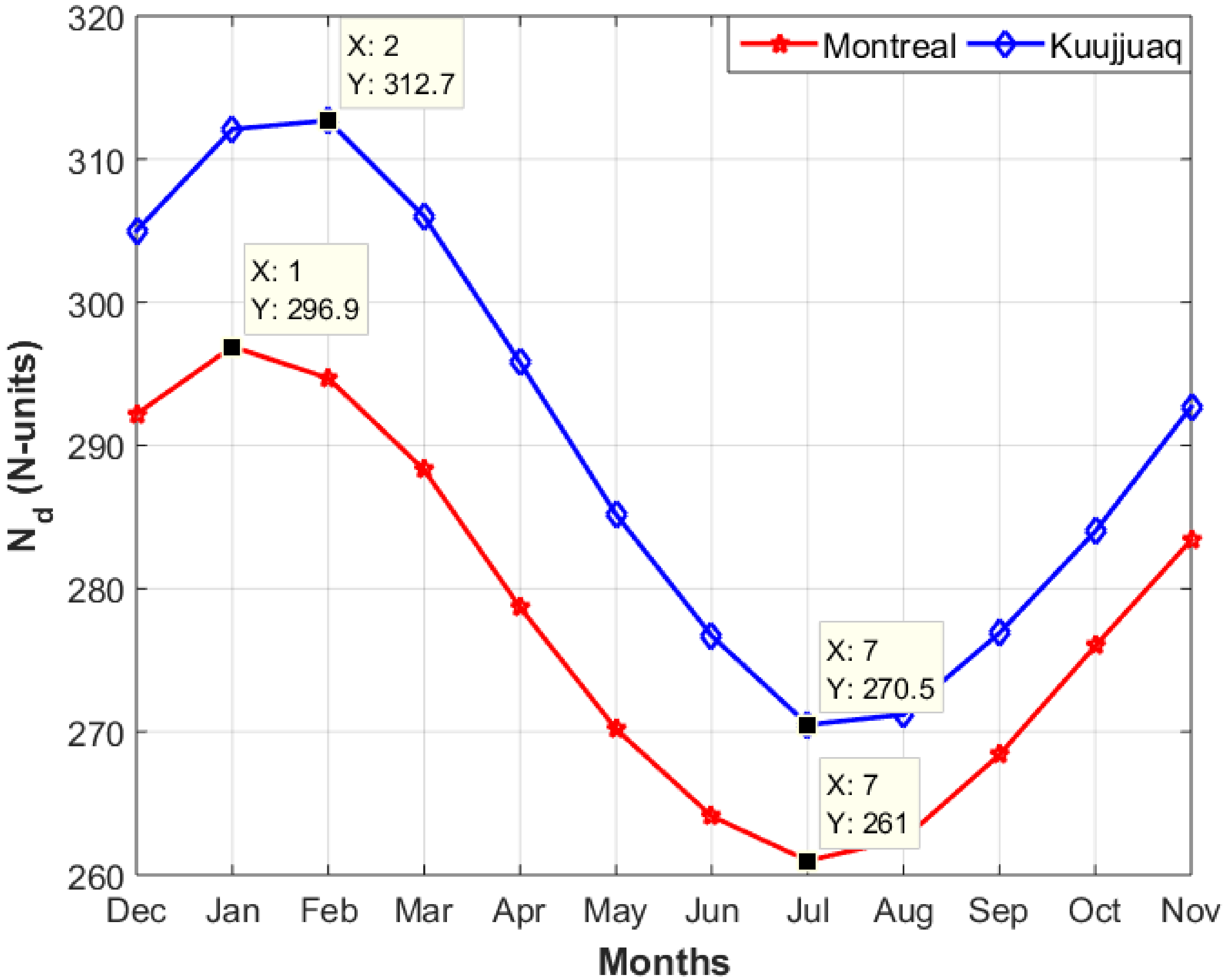

320
310
300
290
280
270
260
X: 2
Y: 312.7
X: 1
Y: 296.9
X: 7
Y: 270.5
X: 7
Y: 261
Montreal
Kuujjuaq
N_d (N-units)
Dec
Jan
Feb
Mar
Apr
May
Jun
Jul
Aug
Sep
Oct
Nov
Months

Figure 2.

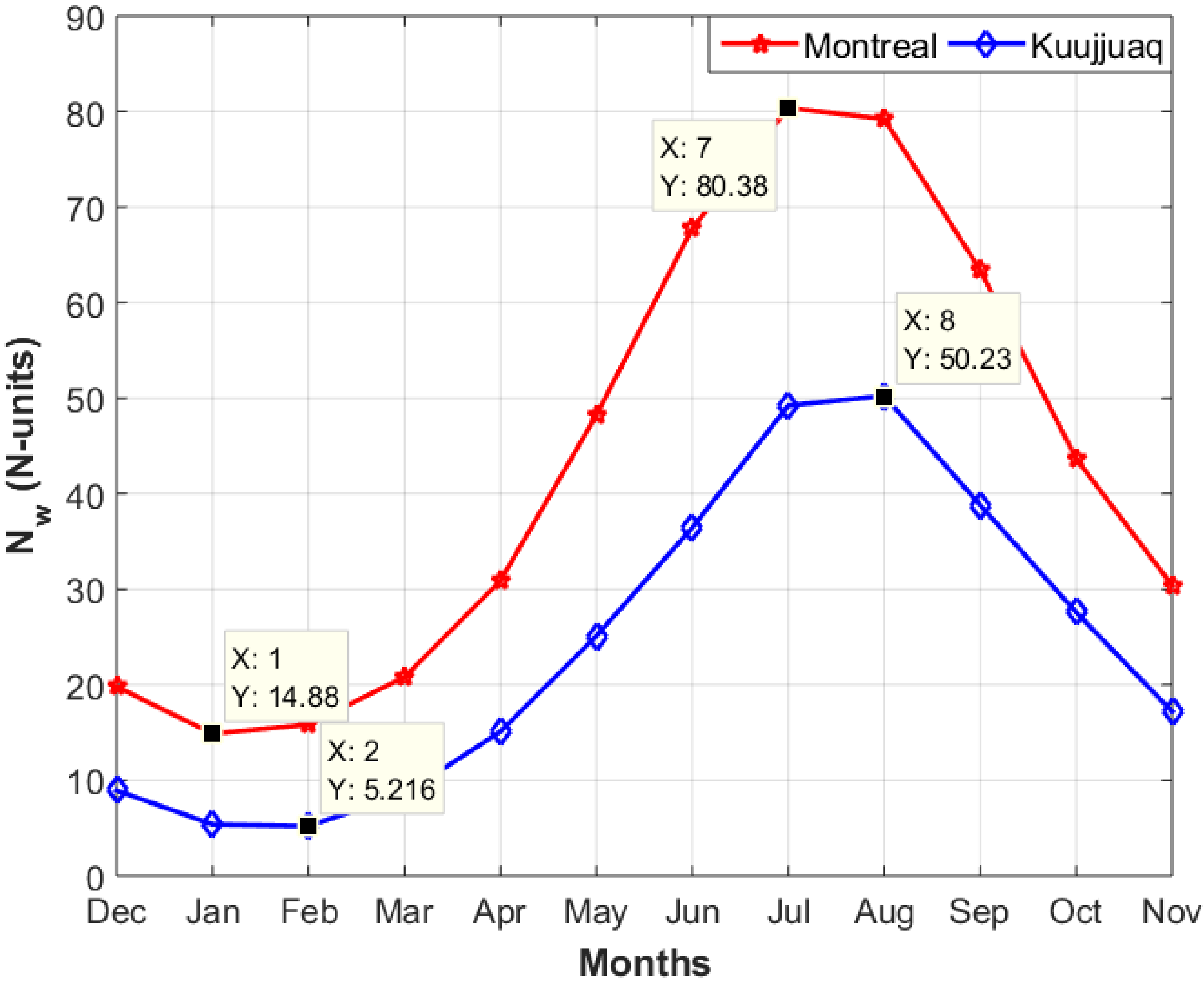

Montreal
Kuujjuaq
X: 7
Y: 80.38
X: 8
Y: 50.23
X: 1
Y: 14.88
X: 2
Y: 5.216
N_w (N-units)
Months
Dec
Jan
Feb
Mar
Apr
May
Jun
Jul
Aug
Sep
Oct
Nov
0
10
20
30
40
50
60
70
80
90

Figure 3.

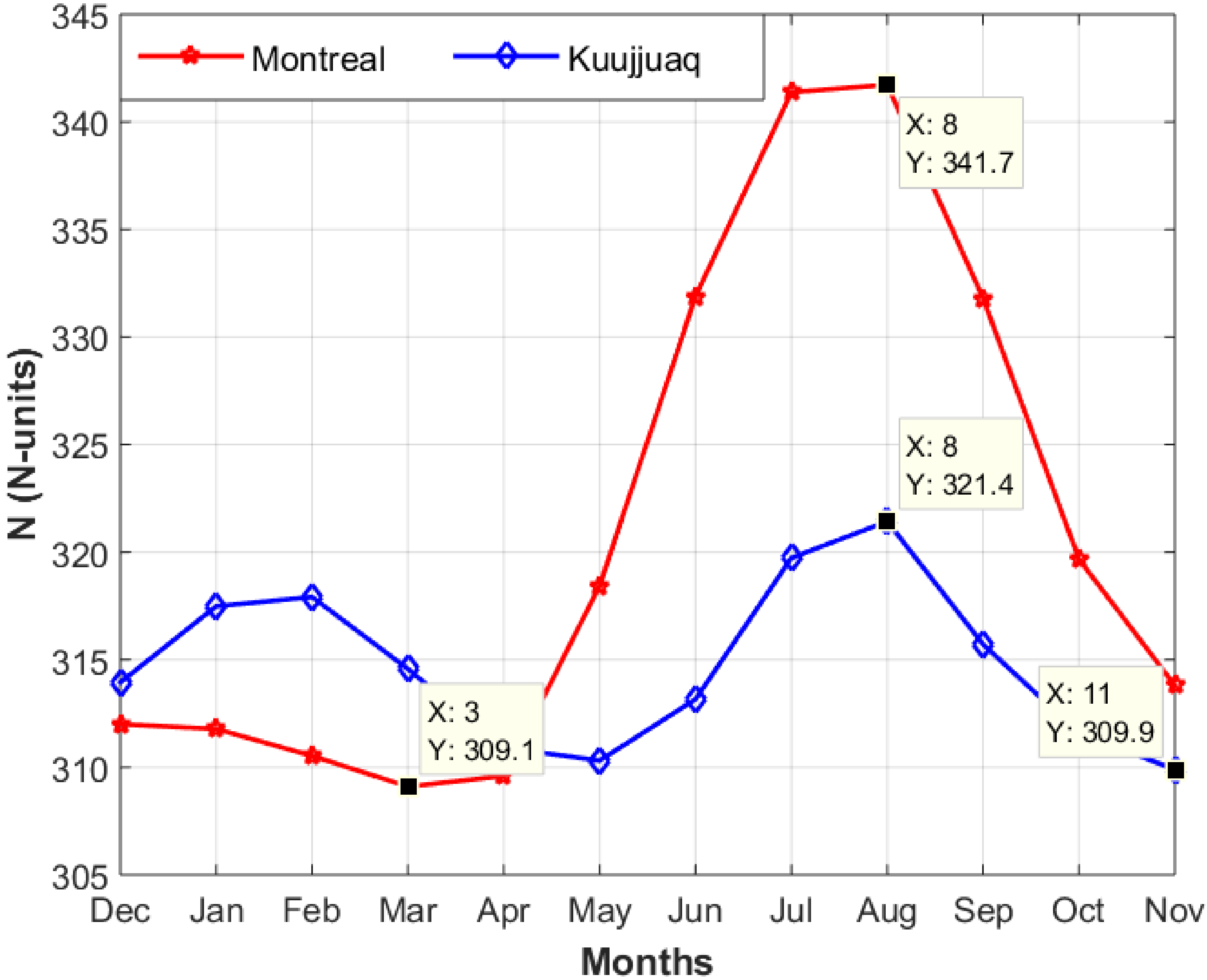

Montreal
Kuujjuaq
X: 8
Y: 341.7
X: 8
Y: 321.4
X: 3
Y: 309.1
X: 11
Y: 309.9
345
340
335
330
325
320
315
310
305
N (N-units)
Dec
Jan
Feb
Mar
Apr
May
Jun
Jul
Aug
Sep
Oct
Nov
Months

Figure 4.

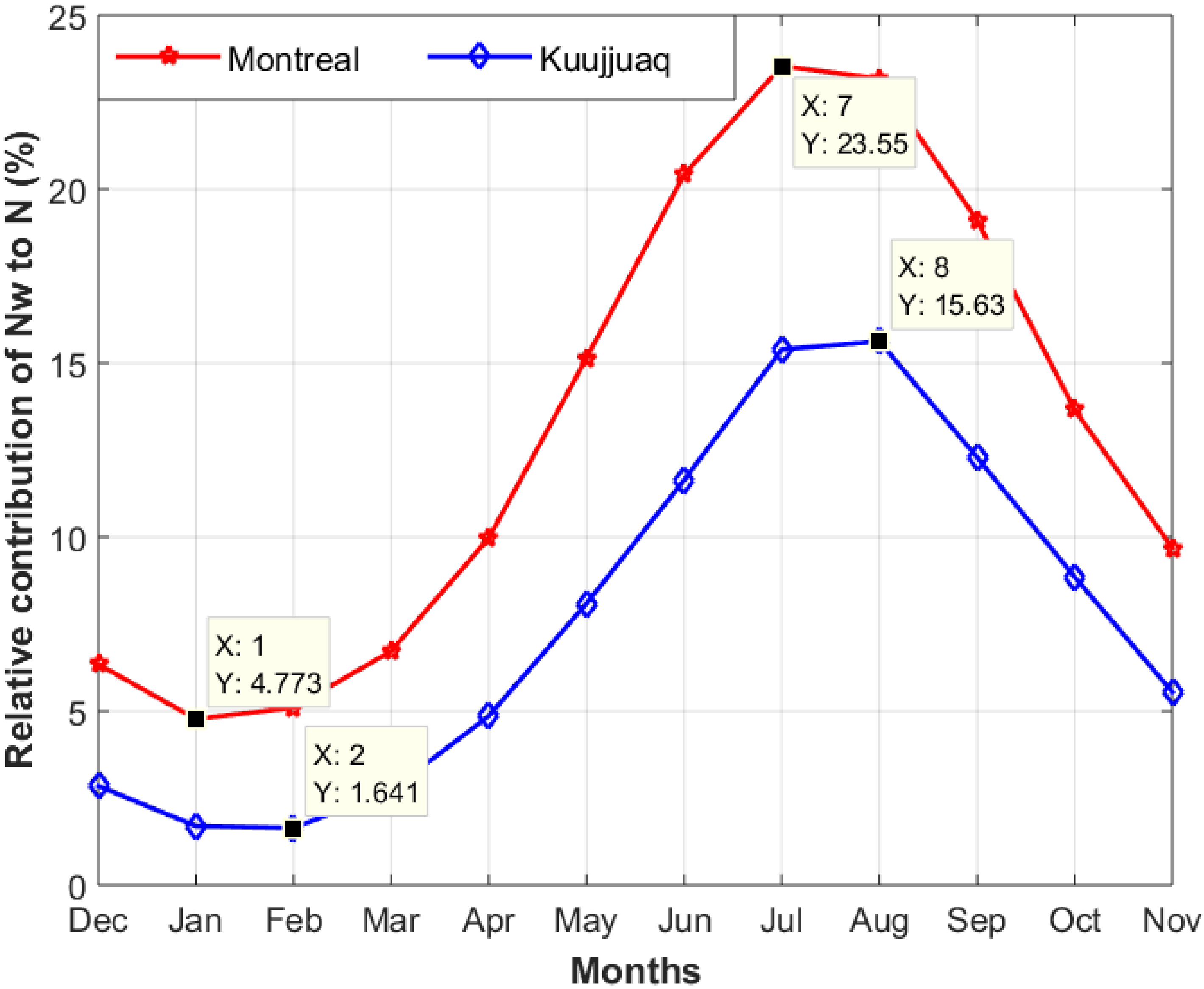

Montreal
Kuujjuaq
X: 7
Y: 23.55
X: 8
Y: 15.63
X: 1
Y: 4.773
X: 2
Y: 1.641
25
20
15
10
5
0
Relative contribution of Nw to N (%)
Dec
Jan
Feb
Mar
Apr
May
Jun
Jul
Aug
Sep
Oct
Nov
Months

Figure 5.

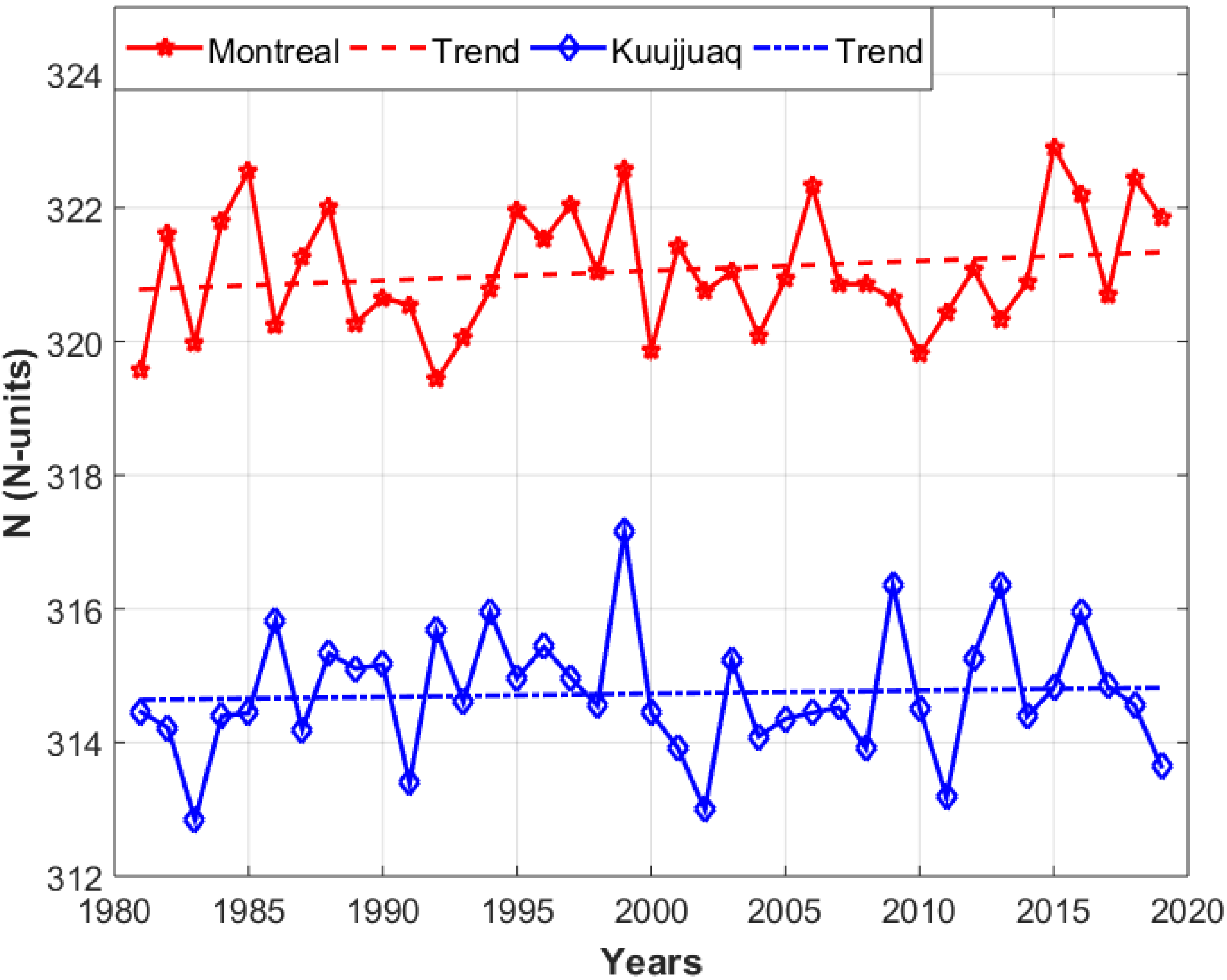

Montreal
Trend
Kuujjuaq
Trend
N (N-units)
324
322
320
318
316
314
312
1980
1985
1990
1995
2000
2005
2010
2015
2020
Years

Figure 6.

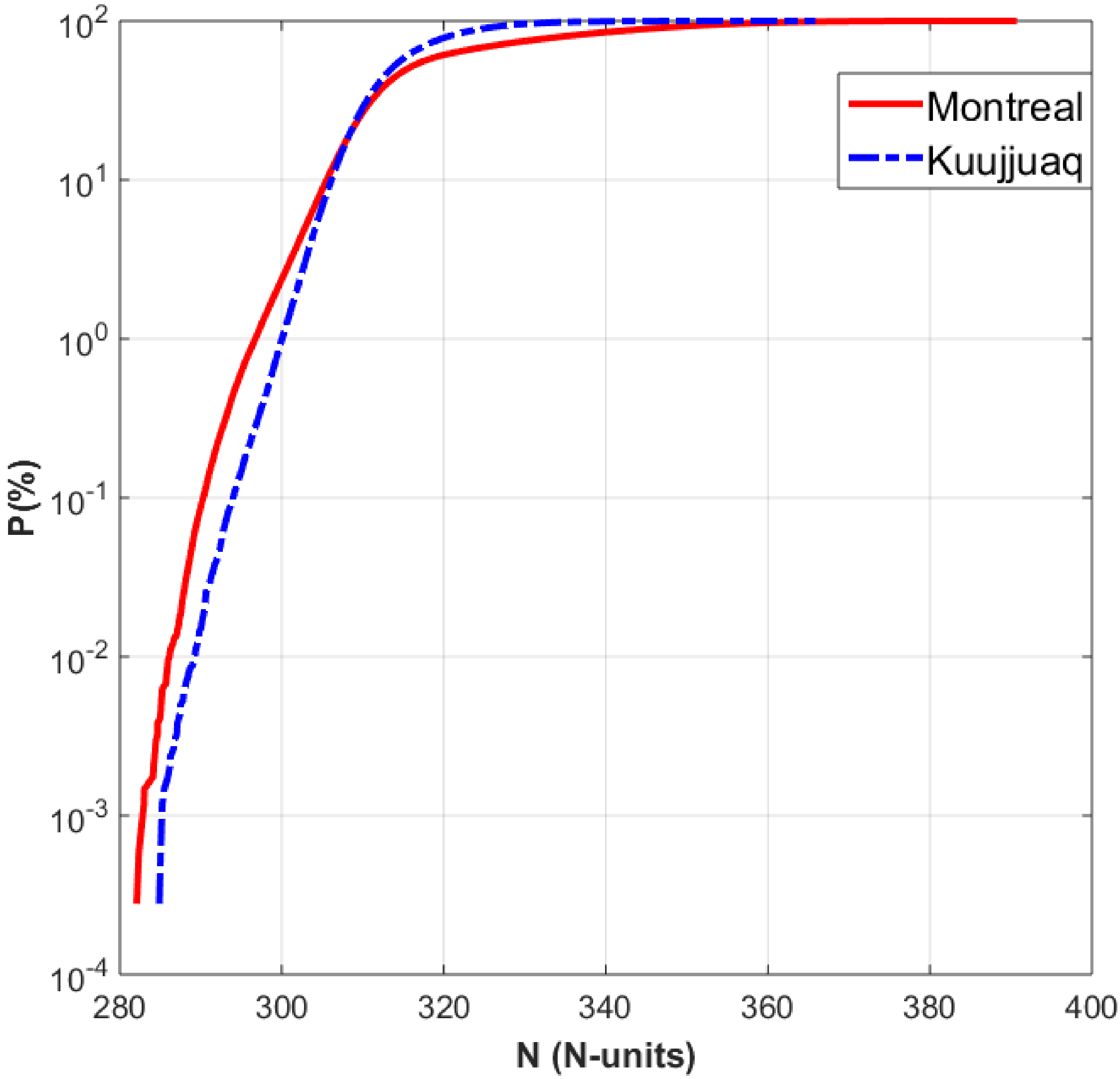

P(%)
N (N-units)
Montreal
Kuujjuaq

Figure 7.

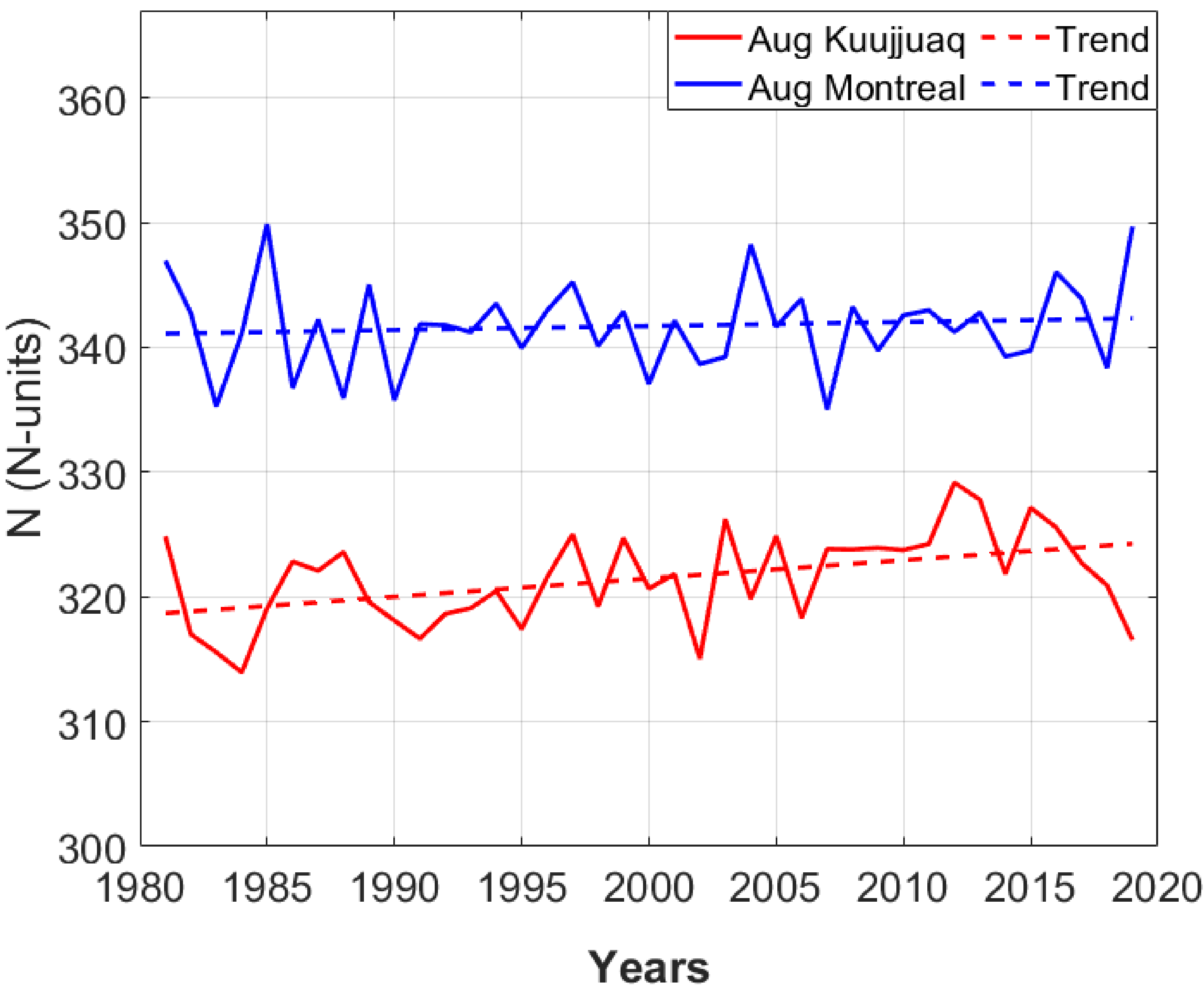
Aug Kuujjuaq
Trend
Aug Montreal
Trend
N (N-units)
300
310
320
330
340
350
360
1980
1985
1990
1995
2000
2005
2010
2015
2020
Years

Figure 8.

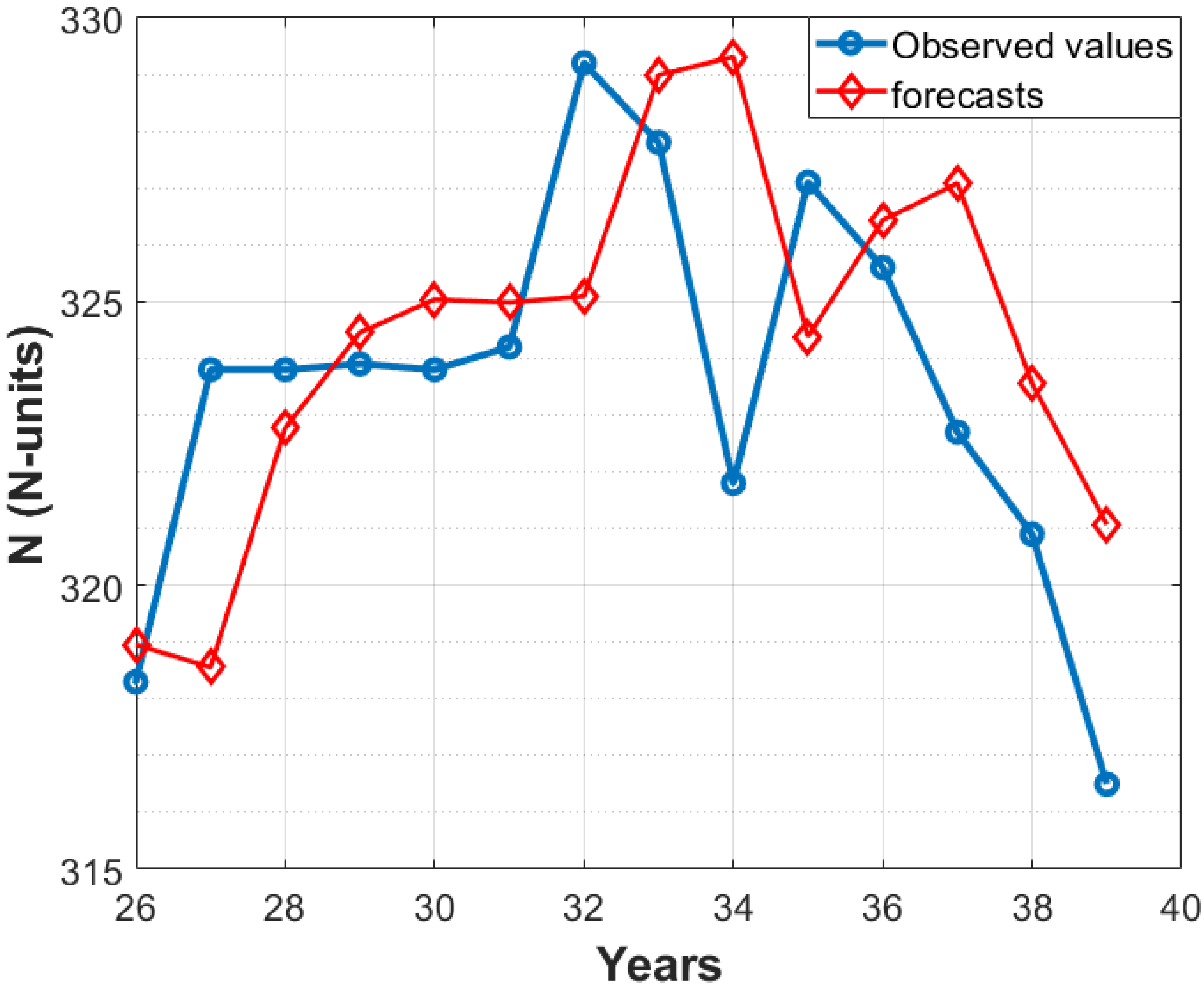

330
325
320
315
26
28
30
32
34
36
38
40
N (N-units)
Years
Observed values
forecasts